Ray Tracing Mirages Using Approximated Ray Paths

Mashhuda Khote and Toby Howard
Department of Computer Science
University of Manchester
Oxford Road
Manchester M13 9PL
United Kingdom

Email: khotem@cs.man.ac.uk

Abstract

There is increasing interest in using computer graphics to model natural phenomena. In this paper we present a technique for modelling mirages.

Natural mirages occur when the temperature profile of the atmosphere causes light rays to bend continuously. The result is a concave ray path, which cannot be easily traced using conventional ray tracing techniques.

This paper presents a physical mirage model which uses an empirical refractive index profile. The model approximates the theoretical ray path by sampling it at intervals and then reconstructing the it. The approximated path is used to ray trace the scene. The results of this work have shown that mirages can be rendered effectively in this way.

1 Introduction

A mirage is a natural phenomenon which occurs when there is a significant temperature gradient in the atmosphere. The temperature profile of the atmosphere has a direct effect on the refractive index profile of that portion of the atmosphere. As the refractive index increases, light rays passing through the medium are bent. The bent light rays fool our visual system and the observed image is not interpreted correctly.

Two of the most frequently observed types of mirage are 'inferior' and 'superior' mirages, and it is with these phenomena that the work described here is concerned.

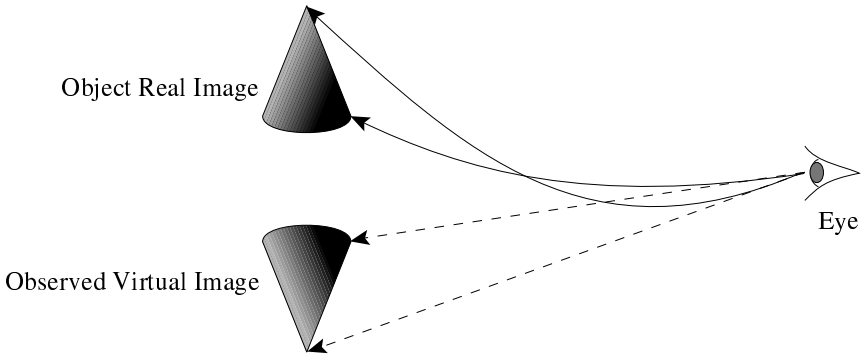

Figure 1: The origin of the real and virtual images in an inferior mirage.

1.1 Inferior mirage

The word mirage almost always brings to mind a particular image: a desert, blazing sun, palm trees and the illusion of water.

These conditions lead to inferior mirages. As the desert sand heats up, it warms the air directly above it by a significant amount relative to the air a few meters above the ground. Thus a temperature gradient is created. The most drastic refractive bending of light rays occurs closest to the ground, where the temperature gradient is changing most rapidly with height. This can result in both a real image and an inverted virtual image of an object being seen. The net effect is similar to observing the scene reflected in water. This is illustrated by Figure 1 which shows two of the rays from a scene which reach an observer's eye together with their apparent point of origin. Both the image and the virtual image may be stretched or compressed vertically, depending on the temperature characteristics of the atmosphere.

Mirage formation also involves total internal reflection, which occurs when a light ray passes into a less dense medium and the angle of incident light is greater than some critical angle. Hence, a complete analysis of mirage phenomena would require integrating the effect of refraction and including some contribution for total internal reflection over the significant range of atmosphere.

1.2 Superior mirage

This type of mirage arises when a surface, such as a frozen-over lake, or snow-covered land is substantially colder than the air above. This produces a temperature gradient as with an inferior mirage, but it is inverted. The ray path is refracted towards the cooler air as before. The resulting image appears to be floating in the sky. This phenomenon is known to sailors as 'looming' and can result in some peculiar visions, such as distant cities floating in the air above

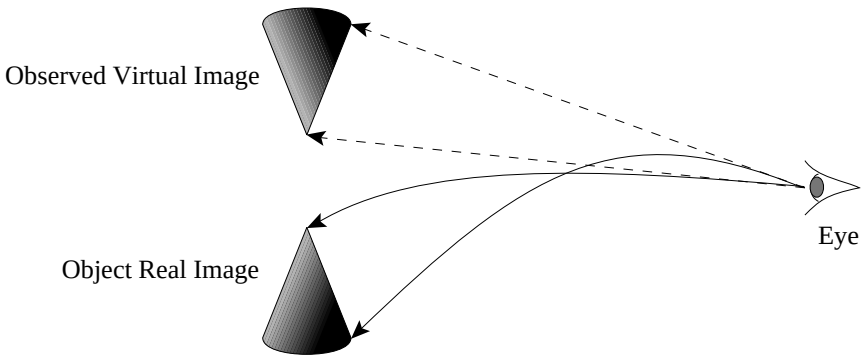

Figure 2: The origin of the real and virtual images in a superior mirage.

lakes [2]. The looming image can be upright or inverted, depending on the distance variation between observer and object, and temperature variations in the air. Figure 2 shows ray paths from an object to an observer along with their apparent point of origin. This type of mirage is far less commonly observed than the inferior mirage.

2 Ray tracing mirages

Ray tracing is a natural approach for modelling mirage effects, although other approaches, such as digital imaging, have also been used (see, for example, [6]). With ray tracing, one possible way to model the temperature profile of the atmosphere is to divide it into discrete bands. This is the approach taken by Berger, Levit and Trout [1], who describe an algorithm devised to render atmospheric refraction using a 'mirage box' object which is placed in front of objects in the scene. Since each band has an associated refractive index, each refracted ray has a new direction vector indicated in Figure 3 by the vectors V_1 to V_5. R is the point of total reflection and P, Q, S and T are points where refraction occurs. Rays are traced such that when the 'mirage box' is the closest object in the scene intersected by a ray, the ray is refracted at each band. The point at which the ray exits the 'mirage box' becomes the origin of a new ray.

This model has some disadvantages. Musgrave [7] draws attention to the fact that the model attempts to simulate a continuous process using a discontinuous approximation. Also, the model relies on placing the 'mirage box' in front of objects, which has an important associated problem which is discussed later.

White [8] suggests that in most real mirages each ray lies in a single plane, giving collinear images. His work is very useful for two reasons. First, he says that the collinearity of images is a result of rays from a point on an object to the observer being in a single plane. Second, he believes that the refractive index

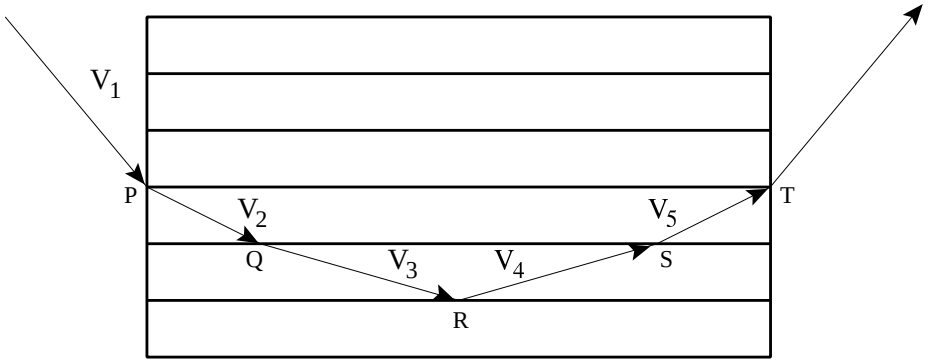

Figure 3: A ray travelling through the 'mirage box'.

profile in the atmosphere remains unchanged by rotation about the vertical axis. Both these ideas are utilised in the new model presented in this paper.

3 A new physical mirage model

Khular et al [5] suggest a mathematical representation of the ray path in a mirage. We use this model to approximate one half of the ray path and then reflect it about the turning point.

Khular et al propose a realistic refractive index profile (for experimental evidence supporting this profile see Fabri [3]). Their derivation of the ray equation relies on one of two refractive index profiles, corresponding to inferior and superior mirages. The refractive index profile giving rise to an inferior mirage is:

$$\eta_y^2 = \eta_0^2 + \eta_1^2[1 - \exp(-\alpha y)] \tag{1}$$

where η_y is the refractive index at a particular height y above the ground, η_0 is the refractive index at the surface, η_1 and α are constants. For a realistic mirage, the atmosphere's refractive index profile uses $\eta_0 = 1.000233$, $\eta_1 = 0.4584$ and $\alpha = 2.303m^{-1}$ giving the graph shown in Figure 4. Khular derives the following differential equation describing the path of a ray:

$$\left(\frac{dy}{dz}\right)^2 = \frac{\eta_y^2}{\eta_p^2 \sin^2 i} - 1 \tag{2}$$

Where η_p is the refractive index at the eye point (z_0, y_0), where the ray makes an angle i with the y axis, as shown in Figure 5. Solving this equation by integrating both sides gives the following equation.

$$\cosh^{-1}\left[k \exp\left(\frac{\alpha y}{2}\right)\right] = \frac{\eta_1 k \alpha}{2\eta_p \sin i}(z - z_0) + \cosh^{-1}\left[k \exp\left(\frac{\alpha y_0}{2}\right)\right] \tag{3}$$

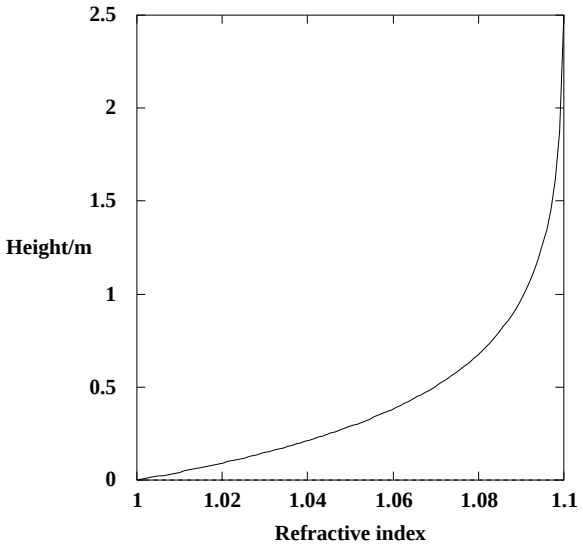

Figure 4: Refractive index η_y as a function of height y.

where η_p and k are given by:

$$\eta_p^2 = \eta_0^2 + \eta_1^2[1 - \exp(-\alpha y_0)] \tag{4}$$

and

$$k^2 = (\eta_o^2 + \eta_1^2 - \eta_p^2 \sin^2 i)/\eta_1^2 \tag{5}$$

The ray path obtained has a minimum at (z_m, y_m), where:

$$y_m = \frac{2}{\alpha} \ln \frac{1}{k} \tag{6}$$

and

$$z_m = z_0 + \frac{2\eta_p \sin i}{\eta_1 k \alpha} \cosh^{-1} \left[k \exp \left(\frac{\alpha y_0}{2} \right) \right] \tag{7}$$

4 The ray-tracing algorithm

The algorithm presented in Khote [4] calculates the ray path taking account of total internal reflection. Hence, at the turning point, bending of the ray path is due to this phenomenon. This is consistent with Khular and Fabri's observations that the ray path is reflected about the turning point and is also in agreement with Musgrave [7].

Since the ray path is only dependant on the z and y components of the left-handed co-ordinate system used, the ray path is the same for any x co-ordinate

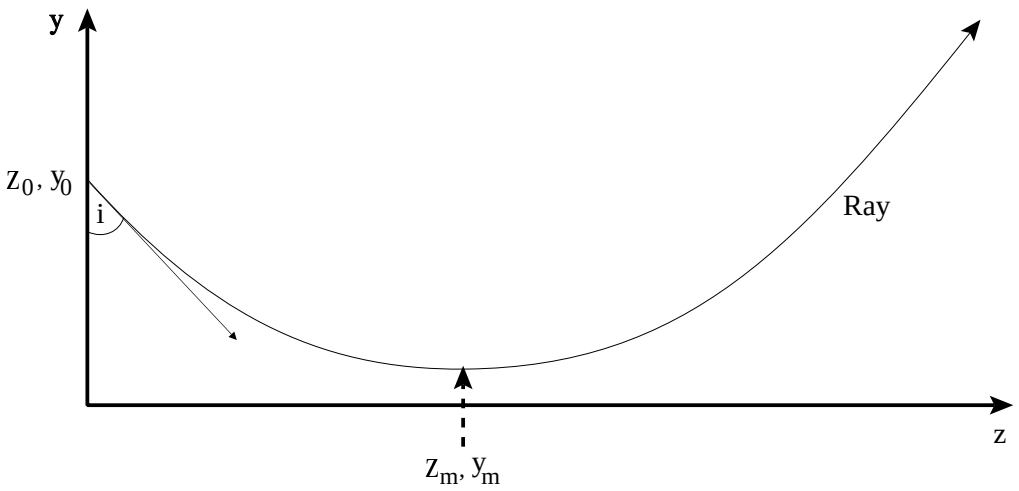

Figure 5: The initial angle i made by the ray.

at a particular height from the ground. Hence, the concave ray path only needs to be computed once for any horizontal scanline. Thus the algorithm performs some precomputation for each scanline:

1. Determine which ray equation to use, depending on whether conditions exist for inferior or superior mirages

2. Compute the angle i made by the vertical y axis and the direction of the initial ray in the appropriate quadrant.

3. Compute the turning point co-ordinate by evaluating k using Equation 5 and substituting it into Equations 6 and 7 to determine z_m and y_m respectively. Transform the origin such that it lies at the turning point, because computation of half of the ray path is performed from the turning point.

4. Adaptively sample the ray path such that the acceptable distance which can be traversed via a linear ray is met. This is performed by choosing an acceptable change in gradient and then evaluating the z and y co-ordinates at this point on the theoretical ray path. y is evaluated using Equations 2 and 1. The z co-ordinate is determined using Equation 3. Figure 6 illustrates the algorithm. The stars on the graph represent samples, the spacing of which depends on the gradient of the curve. y is the height axis, z is the axis into the screen.

5. Reflect the ray path about the turning point to obtain the concave shape over the sampled area of the ray path.

6. Set up the master curve by assigning the respective end points of the ray path to some arbitrary large positive and negative values. Note that: beyond the critical bend in the ray path, the ray can be assumed to be linear.

7. Find the z, y co-ordinates of the eye on the master curve, then set one extreme of the curve to these co-ordinates and discard all the points behind the camera.

8. Convert the final ray path into a set of vectors.

9. For each pixel:

   (a) Rotate the ray path about the eye so that it lies in the correct x plane. This is shown in Figure 7.

   (b) Trace the theoretical ray path by shooting a ray vector from the eye to the sample point beyond. If it reaches this point, shoot a ray to the next sample point and so on, following the ray path until the ray intersects an object or is culled.

5 Results

Colour slide 5.1 shows a test scene used, with two identical partially reflective spheres positioned at the same z, y co-ordinates. Colour slide 5.2 illustrates the same scene rendered with the inferior mirage atmosphere. There is some vertical distortion seen in both the real and virtual images due to the properties of the mirage atmosphere. In real mirages there is almost always some vertical distortion seen, so it is fair to expect the same from our model. For a comparison we have included a photograph of an actual superior mirage in Western Australia. Vertical distortion of the virtual image can clearly be seen in the photograph.

6 Conclusions

In this paper we have presented a new approach to modelling inferior and superior mirage phenomena, which is more closely based on theoretical analysis than the simple 'band' model, and considers the mirage as being created by properties of the atmosphere. The model has performed well in practice, and the mirage computation can be readily included in standard ray tracing algorithms.

The most significant difference between the model described and Berger et al's approach is that the atmospheric characteristics for mirage formation are an integral part of the model. This has the consequence that it is possible to walk towards the mirage and it will disappear. However, a consequence of the scanline method used is that the eye cannot be tilted from the vertical.

Possible directions for further work could be to use this model in a Virtual Reality application. The atmosphere as it stands is static so turbulence could be incorporated into the model by 'randomly walking' the ray path by some very small value.

Acknowledgements

It is a pleasure for us to thank Professor F. Kenton Musgrave and Dr. Alan Murta, for their support and advice on the work described in this paper.

References

[1] Marc Berger, Terry Trout, and Nancy Levit. Ray tracing mirages. *IEEE Computer Graphics and Applications*, 10(6):36 – 41, May 1990.

[2] Marc Berger, Terry Trout, and Nancy Levit. Rendering mirages and other atmospheric phenomena. In *Proceedings Eurographics*, pages 459 – 468. Elsevier Science Publishers B.V. (North-Holland), 1990.

[3] E. Fabri, G. Fiorio, F. Lazzeri, and P. Violino. Mirage in the laboratory. *American Journal of Physics*, 50(6):517 – 521, June 1982.

[4] M. Khote. Modelling natural meteorological phenomena. Master's thesis, University of Manchester, October 1993.

[5] E. Kular, K. Thyagarajan, and A.K. Ghatak. A note on mirage formation. *American Journal of Physics*, 45(1):90 – 92, January 1977.

[6] W. H. Lehn and W. Friesen. Simulation of mirages. *Applied Optics*, 30(24):1267 – 1273, August 1991.

[7] F. Kenton Musgrave. A note on ray tracing mirages. *IEEE Computer Graphics and Applications*, 10(6):10 – 12, November 1990.

[8] R. White. Mirage: Multiple images. *Applied Optics*, 29(22):3204 – 3206, August 1990.

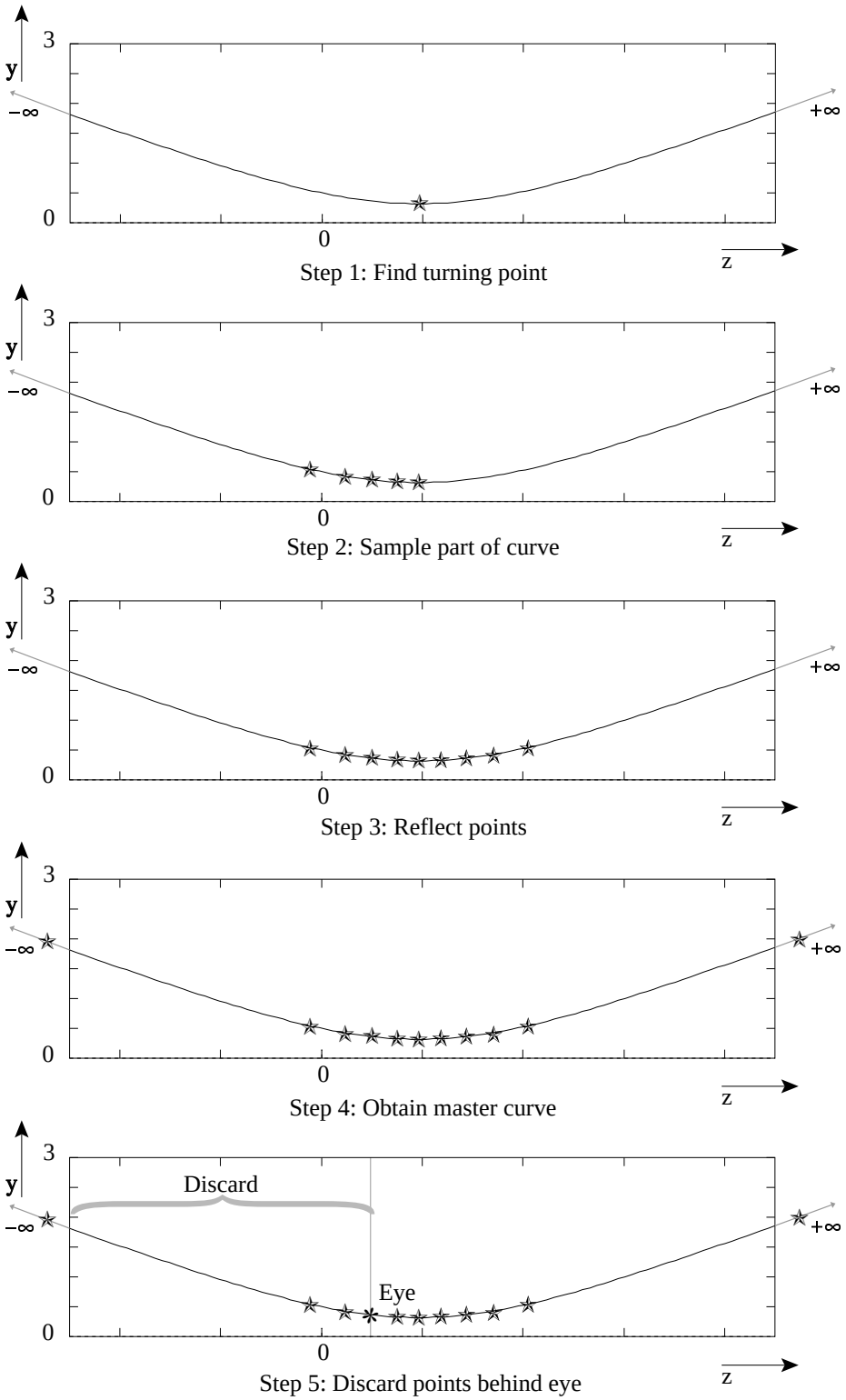

Figure 6: Progressive steps for sampling a ray path.

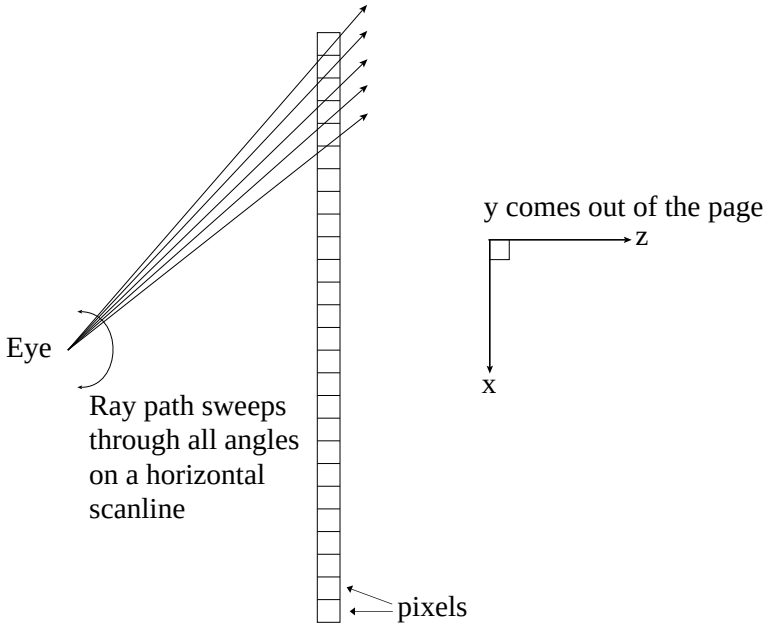

Figure 7: Rotating the ray path through each pixel.